Available online at www.sciencedirect.com
ScienceDirect
C. R. Physique 8 (2007) 426–437
COMPTES RENDUS PHYSIQUE
http://france.elsevier.com/direct/COMREN/

Optical techniques for direct imaging of exoplanets/Techniques optiques pour l'imagerie directe des exoplanètes

Comparison of ELTs, interferometers and hypertelescopes for deep field imaging and coronagraphy

Antoine Labeyrie [a,b]

[a] *Collège de France, 11, place Marcelin Berthelot, 75231 Paris cedex 05, France*
[b] *Observatoire de Calern, 06460 Caussols, France*

Available online 7 June 2007

Abstract

We compare the science potential of ELTs, interferometers and hypertelescopes having the same collecting area. Hypertelescopes with hundreds or thousands of small apertures overcome the 'field crowding' problem which interferometers have for aperture synthesis with few apertures. They also improve the signal/noise ratio as $N^{7/4}$ if N is the number of apertures. With a modified laser guide star scheme, currently being explored, they become, in principle, suitable for observing deep fields of remote galaxies, with a limiting magnitude identical to an ELT, and with higher resolution. Before initiating major ground-based projects, the comparison of these architectures should be studied in more detail, for the various observing targets and science cases. ***To cite this article: A. Labeyrie, C. R. Physique 8 (2007).***

Résumé

Comparaison des ELTs, interferomètres et hypertélescopes pour l'imagerie des champs profonds et la coronographie. On compare le potentiel de science des ELTs, interferomètres et hypertélescopes ayant la même surface collectrice. Des hypertélescopes ayant des centaines ou milliers de petites ouvertures surmontent le problème d'encombrement des champs qui affecte les interféromètres ayant peu d'ouvertures. Ils améliorent aussi le rapport signal/bruit comme $N^{7/4}$, N étant le nombre d'ouvertures. Avec une étoile guide laser modifiée, étudiée actuellement, ils permettront en principe d'observer des champs profonds de galaxies lointaines, avec une magnitude limite identique à un ELT, mais une meilleure résolution. Avant d'engager de grands projets au sol, il importe de d'étudier en détail la comparaison de ces architectures, pour les différents programmes d'observation. ***Pour citer cet article : A. Labeyrie, C. R. Physique 8 (2007).***

Keywords: Hypertelescope; Coronagraphy

Mots-clés : Hypertélescope ; Coronographie

1. Introduction

The emergence of stellar interferometers having many apertures spaced far apart, and capable of providing snapshot images with a rich information content, opens a new path for astronomical observing, from Earth and in space.

E-mail address: labeyrie@obs-hp.fr.

1631-0705/$ – see front matter
doi:10.1016/j.crhy.2007.03.003

The imaging properties of these new instruments, called 'multi-aperture densified-pupil dilute interferometers' or 'hypertelescopes' have been discussed by several authors (Labeyrie [1], Pedretti et al. [2], Gillet et al. [3], Lardiere et al. [4]) for normal and coronagraphic observing. Forms of implementation considered vary from homogeneous arrays to 'out-rigger' arrays associated to large telescopes or groups of telescopes. Design concepts vary from arrays of telescopes to arrays of mirrors, spherical or paraboloidal, including the option of fiber-optical links (Patru et al. [5]).

Here, we compare the performance of such instruments having different sub-aperture counts and dilutions, their total collecting area being assumed equal, as well as the angular resolution, when comparing interferometers. Two or three rather large apertures, exploited as an aperture synthesis imaging interferometer with baseline much longer than the sub-aperture size, are thus compared with hypertelescope arrays having many apertures of much smaller size. The case of a single aperture, in the form of an ELT, is also considered, in spite of the much lower resolution, and its expected science impact compared to that of few-element interferometers and the 'diluted ELTs' buildable in the form of rich hypertelescopes. Coronagraphy is also considered in the comparison.

2. Four possible evolutionary paths for terrestrial optical instruments

Four main evolutionary paths can be foreseen for ground instruments, toward higher limiting magnitudes, resolution and the extreme dynamic range needed for exoplanet imaging: (i) ELTs; (ii) Aperture synthesis imaging with a few ELTs, interferometrically coupled; (iii) Rich dilute arrays of many small apertures, with total collecting area comparable to an ELT but much higher resolution; (iv) ELT(s) coupled with many smaller 'outrigger' apertures, the total collecting area of which is much smaller, but which provide hypertelescope imaging at much higher resolution than with an ELT alone. In space, the third path is likely to become dominant if rich formation flights become feasible.

2.1. ELTs

Following the Keck I and II telescopes, current studies of the TMT and the E-ELT suggest their feasibility, while identifying a number of difficult points. Among these, the critical issue of adaptive optics, its sky coverage and its performance for extreme coronagraphy are not completely clarified.

2.2. Two or three ELTs for aperture synthesis

This is similar to the existing interferometry modes of the Keck telescopes and the VLT. Because even larger ELTs are unlikely to be movable, the aperture synthesis process exploits the Earth's rotation. As will be discussed in Section 4, the performance of image reconstruction by aperture-synthesis does not reach that of many-aperture systems (type 3 and type 4) having the same collecting area.

2.3. The hypertelescope, a diluted form of ELT

The benefits of diluting ELTs, such as the American TMT and the European E-ELT, have been previously discussed: hundreds of mirror elements can be arranged as a dilute array spanning 500 m to possibly 1.5 km at suitable concave sites. The snapshot image provides the same limiting magnitude, if properly phased, and a higher resolution. Pupil densification, which makes the difference between Fizeau imaging and hypertelescope imaging, greatly improves the sensitivity if the camera is not photon limited.

As discussed in Section 3.1, the classical field-crowding limitation of interferometers is so much relaxed with the numerous apertures (Lardière et al. [4]) that deep-field imaging is possible on faint galaxy clusters, and a rather wide field is accessible by using an array of pupil densifiers in the focal combiner, as sketched in Fig. 1.

Practical design concepts in this class of instruments are of three types: (i) planar array of telescopes, requiring moving telescopes or as many long delay lines if their high cost can be funded; (ii) paraboloidal arrays, requiring no delay lines, but which must be globally pointed. This may be feasible in the form of the Perce-Neige concept proposed for Dome C, with mirrors carried by a large net suspended from balloons. Much further engineering assessment is, however, needed to qualify such concepts; (iii) spherical arrays require concave sites where mirrors can be anchored to the bedrock. The test results of the Carlina-1 prototype (Le Coroller et al. [6]) have partially demonstrated the feasibility of such hypertelescopes. A larger Carlina-2 version, expected to provide effective apertures beyond 100 m, is under study.

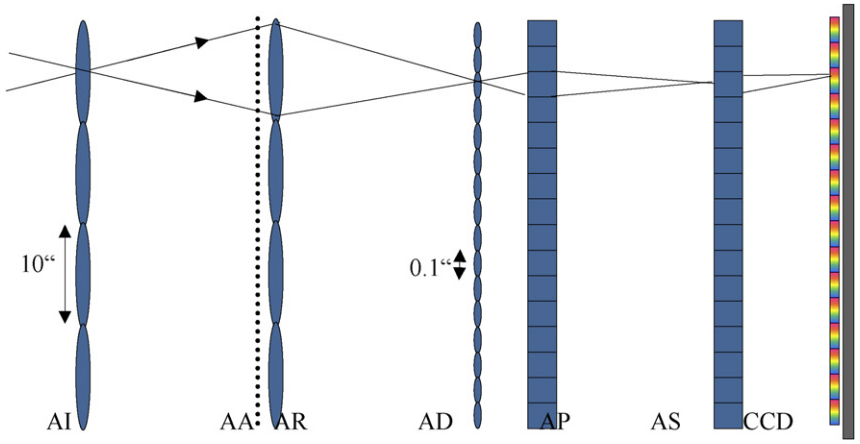

Fig. 1. Multi-field imaging and adaptive optics for a hypertelescope: AI—Fizeau focal plane containing an array of field lenses, with pitch matching the isoplanatic patch; AA—pupil plane array of triple actuators correcting tip-tilt and piston errors in each isoplanatic patch; AR—array of lenses relaying corrected Fizeau images of each patch; AD—array of micro-scale field lenses, with pitch matching the diffractive envelope; AP—array of micro-scale pupil densifiers; AS—array of micro-scale spectro-imagers also serving for piston analysis; CCD—detector array. The pitch of the AD, AP and AS arrays is identical, thus producing separate spectro-imaging channels within adjacent envelope fields. AS focuses a series of spectra on the detector CCD, one for each speckle of the image formed in each channel. Residual field aberrations of the large up-stream optics are also correctible with deformed AR lenses and thickness variations among the AP lenses. Integrated optics is needed for a manageable instrument size. The thousands of narrow DIFs which can be simultaneously spectro-imaged are separated by gaps on the sky, but they can be filled, for stitching a continuous image, with a sequence of offset exposures.

2.4. Hybrid array: ELT with out-rigger hypertelescope

A Fizeau interferometer can have many sub-apertures of unequal sizes. The interference function is unaffected, but the sub-images have envelopes of different sizes. As discussed by Labeyrie [7], this can be corrected in a densified pupil by performing unequal amounts of pupil densification. It does not affect the field invariance of the interference function.

Is this of interest for achieving hypertelescope arrays with many small apertures and one or more large ones? Conceivably, an ELT could thus be combined with a much larger array of many smaller apertures. Numerical simulations of direct images obtained in this way, with unequal pupil densification, give interesting results: the interference peak, sized as λ/D, can remain strongly dominant even if the combined collecting area of the small apertures is much less than that of the large aperture(s). This synergy provides the resolution of the large diluted array and the luminosity of the ELT, more compact but having much more collecting area. It justifies a more detailed assessment, especially regarding the science impact, and design concepts toward practical associations of ELTs and hypertelescopes.

Among the possible practical designs, those involving an ELT at the edge of a crater or deep valley have the advantage of requiring no long delay line. Indeed the spherical locus of the hypertelescope, according to the Carlina concept, can then be positioned to contain the ELT's mechanical node, where a small mirror can reflect its light beam toward the focal gondola of the hypertelescope. Such an arrangement appears feasible at sites such as the Roque de las Muchachos observatory (La Palma, Canarias) which dominates the large extinct caldera of the Taburiente, a possible nest for a large Carlina hypertelescope, to be coupled with an ELT residing at the edge (Labeyrie [7]).

At smaller scales, the slopes of a peak carrying an ELT could carry many 'out-rigger' mirrors or telescopes, but this would require many delay lines, as would also be the case for such arrangements on a flat site. Optical fibers linking the telescopes cannot help much in this respect, since they do not alleviate the need for delay lines, although their use for densified-pupil imaging has been verified in the laboratory by Patru et al. [5].

3. Compared performance of ELT, aperture synthesis and hypertelescope imaging

Comparing the science potential of ELTs and hypertelescopes, at equal collecting area, requires a discussion of magnitude limits, of field crowding in the latter, and of coronagraphic performance. We show below that the limiting magnitude is in principle identical if both types of instruments have adaptive optics.

3.1. Crowding and limiting density of 'active resels'

Let us begin by considering a many-aperture, diluted, phased Fizeau array and the direct image which it produces. There is a spread function, which typically has a central peak amidst a broad halo. If the array is periodic, with square or triangular pitch, the halo itself contains a 'reciprocal' array of periodic peaks dominating a darker background. In white light, these become radially dispersed toward the white central peak, since the periodic aperture then behaves as a crossed diffraction grating. If disorder is progressively introduced in the periodic aperture pattern, by randomly moving the apertures, the white central peak is unaffected but the halo peaks become attenuated, and then vanish among chromatic speckles which appear between them. Within the broad speckled halo, there remains a darker zone extending from the central peak to a λ/s radial extent, if s is the average spacing of the apertures (Patru et al. [5], Lardière et al. [4]). Its energy deficiency, with respect to the speckled halo obtained in the absence of phasing, equals the energy content of the central peak. Within the peripheral speckled halo, the average peak/speckle ratio of intensity is of the order of N, the number of apertures. If the phasing is disturbed, the peak and dark zone vanish into a uniform speckled halo filling the diffractive envelope.

Upon densifying the pupil, for intensifying the image according to the hypertelescope scheme, the snapshot image covers a smaller sky patch, of size λ/s, but the crowding limit of N^2 stars per λ/d patch still holds, where d is the size of a sub-aperture, although the snapshot image then cannot show as many stars. Down to N stars only are distinctly imaged if the array is periodic and the pupil fully densified. As discussed in Section 3.3, wide fields can be imaged sparsely, 'grid-wise', if adjacent λ/d sky patches are fed to separate densifiers.

Large hypertelescopes, comparable in collecting area to an ELT, are expected to have a comparable sensitivity for imaging deep fields and other extended objects having many emissive or 'active' resels. This is beyond the capabilities of interferometers having few apertures, but the numerous apertures of those belonging to the hypertelescope class improves their performance in this respect.

The limiting density of 'active resels' on the sky can be calculated by considering the observed field as a random constellation of point sources having equal luminosities. If $A = \pi N d^2/4$ is the total collecting area, which we assume constant for comparing the crowding limit when N is varied, it has been shown (Lardière et al. [4]) that, in the non redundant case, the maximal number R of active resels per diffractive envelope is

$$R = N^2 = 16A^2/\pi^2 d^4$$

However, the sky solid angle of this diffractive envelope, defined by the sub-apertures, is $\pi(\lambda/d)^2/4$, so the maximal density of 'active resels' per sky area (in steradian), is:

$$\sigma_s = 4R/\pi(\lambda/d)^2 = 4N^2/\pi(\lambda/d)^2 = 64\pi^{-3}A^2 d^{-4}\lambda^{-2}d^2 = 64\pi^{-3}A^2 d^{-2}\lambda^{-2}$$

Per square arc-second, the maximal density of 'active resels' is:

$$\sigma_{\mathrm{as}} = 1.4 \times 10^{-9}\pi^{-3}A^2 d^{-2}\lambda^{-2}$$

It improves as the inverse area of each sub-aperture, indicating a marked advantage for more numerous and smaller apertures. Interestingly, it does not depend on the global array size D: enlarging a given array by spreading apart its apertures thus improves the resolution without degrading the crowding limit, expressed as the limiting number of 'active resels' per sky area. However, in a given observed field, improving the resolution tends to create more 'active resels' if multiple stars or galaxies become resolved, and this can limit the useful array span if no apertures are added.

As an example, with a collecting area of 1000 m^2, at visible wavelengths, the crowding limit is 1.5 billion resolved stars per square arc-second if there are 16 000 sub-apertures of 25 cm, or 95 million stars per square arc-second if there are 1000 sub-apertures of 1 m, or 1.5 million stars per square arc-second if there are 16 sub-apertures of 8 m.

The same calculation indicates that a single aperture of 31.6 m has a crowding limit of 95 000 stars per square arc-second. This indeed corresponds to the number of adjacent Airy peaks filling a square arc-second, showing that the crowding limit calculated above also applies to conventional telescopes. Any stars in excess are necessarily overlapping their Airy peak with that of others. It makes them thus unresolvable, but does not degrade the image contrast in this particular case of monolithic apertures.

3.2. Moving apertures extend the crowding limit of hypertelescopes

We again consider a dilute, many-aperture Fizeau arrangement which is phased. The spread function has a central peak and weaker speckled side lobes filling the halo. Moving the apertures does not much affect the peak, but changes the speckle pattern, so that a long exposure made while the apertures are moved will show a much smoother halo around the same central peak, or peaks, if there are several stars. The faint companion of a star is then better detected against the smoothed halo, unless photon noise makes it easier to detect a very faint companion against a dark speckle. A cluster of many stars located within the envelope extent gives an image where the peaks emerge better from the smooth superposed halos. Obviously more stars can be detected than with static apertures, since the speckle residues are better attenuated.

If the aperture is periodic, and remains so while being varied, the secondary peaks replacing the speckles also tend to form a smooth halo, where central peaks from multiple stars may remain detectable. The effect naturally occurs in periodic Carlina hypertelescopes since the pupil rotates significantly during exposures lasting hours. The crowding limit, calculated in Section 3.1, which assumed a fixed aperture, is therefore pessimistic in this respect.

3.3. Extending the hypertelescope field of view with arrayed densifiers

The 'Direct Imaging Field' (DIF) of hypertelescopes covers only a small part of the sky patch matching the diffractive envelope of its sub-apertures. However, many such adjacent patches can be observed in parallel, using as many separate pupil densifiers (Fig. 1). Spectra of each speckle are provided by spectro-imagers, as will be discussed in Section 7.2.

With hundreds of apertures, and multi-field focal optics such as shown in Fig. 1, 'stitched' images can thus be assembled from a sequence of slightly offset exposures. As an example, 1000 sub-apertures of 1 m, spaced 30 m apart, comparable in collecting area to a 30 m ELT but having 30 times higher resolution, provide, at visible wavelengths, DIF sizes of 3 mas, containing 30×30 resels, located within diffractive envelopes of 100 mas. With an array of 200×200 densifiers filling 20×20 arc-seconds, 40 million resels can be imaged simultaneously. 40 billion resels can be assembled into a continuous image through a stitching sequence of 1000 offset exposures.

The size of the multi-densifier array is limited in practice by the field aberrations, coma and astigmatism of the upstream Fizeau optics, although some correction for these aberrations can be incorporated in each micro-scale densifier by adjusting the thickness of its lenses. Aberrations, if expressed as wavefront errors, scale as the size of a telescope, for a given optical design and field angle. If the visible diffraction-limited field of the 40 m E-ELT is two arc-minutes, then a 25 times larger version, spanning 1000 m and exploited as a hypertelescope, is diffraction limited in the same field at a 25 times longer wavelength in the infra-red. In the visible, the diffraction-limited field shrinks to 5 arc-second if coma is the dominating aberration. A somewhat larger field may thus be expected for a 1000 m hypertelescope of similar design, if adequate optical path corrections are incorporated in each densifier as required to locally correct the field aberrations.

The Carlina architecture for hypertelescopes can further enrich the observing throughput, and corresponding science, by using several sets of focal optics, independently positioned on the focal sphere. This is more easily feasible in space, where many such focal stations can be built in the form of separate satellites having their own position control system, but Earth-based mechanical solutions involving cables and winches at deep valley sites can probably also accommodate a dozen foci which can be equipped for distinct science programs.

4. Compared sensitivity of aperture synthesis and hypertelescope

Nakajima [8] discusses in detail the compared sensitivity of 'pairwise' and 'all-in-one' beam combinations, corresponding to aperture synthesis and the Fizeau or hypertelescope, for a N-element interferometer. He expresses some disagreement with previous articles on the subject by Kulkarni et al. [9], Ridgway and Roddier [10]. Here, the issue is discussed from a hypertelescope point of view, and different conclusions are also reached. Like Nakajima, we assume that the array is non-redundant and ideally phased.

The comparison of sensitivity for hypertelescope and aperture-synthesis interferometers can be made conveniently by building the latter as a masked version of the former, optically identical, with the same photon-limited camera, except for the presence of a mask selecting pairs of apertures in sequence. For aperture synthesis, the pair-wise fringes are recorded on the camera as sine fringes, either Fizeau-type or Michelson-type depending if the pupil densification

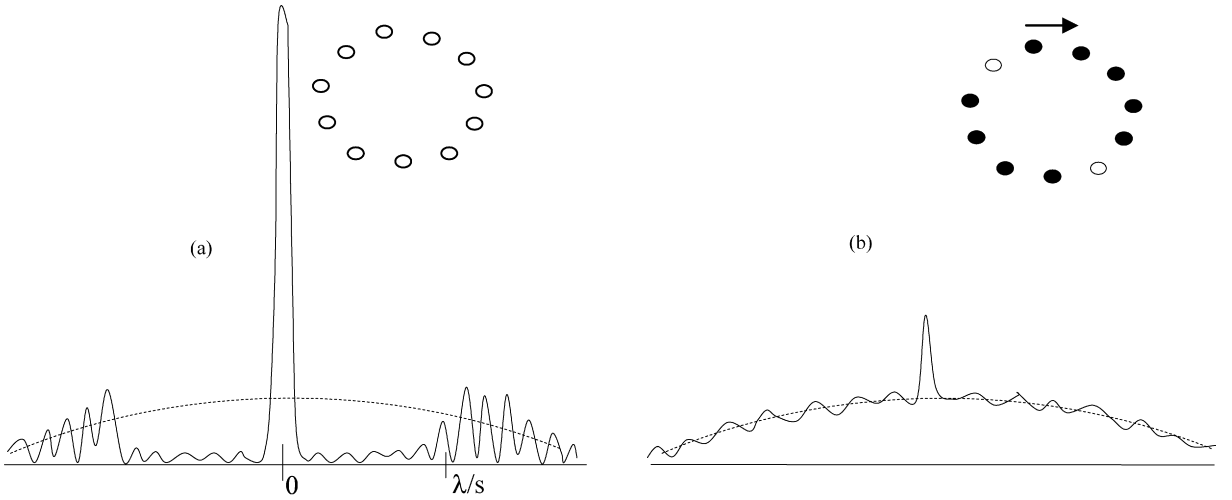

Fig. 2. Sketch of Fizeau image profiles with: (a) many apertures combined all-in-one; (b) the same apertures combined pairwise, with all aperture pairs unmasked in sequence and the images added. Each pair gives sine fringes, forming low contrast speckles when added, except on axis where a peak remains at twice the average halo level. The difference of both profiles results from the coherent vs. incoherent addition of vibrations. For a fair representation of the peak intensity gain in (a), amounting to $N/2$ at equal collecting area and observing time, profile (a) is attenuated by a factor $2/N$. In both cases, the speckles can be further smoothed by adding images formed with different aperture patterns. The spread function being well calibrated or calculated, a planet's peak in the halo is detectable if its level exceeds the local photon noise from the star. The higher peak and fainter dark zone of the all-in-one combination makes it more sensitive. For faint planets, a similar coronagraph can be attached in both cases, with different masks. If their star residues are similar, the more intense planet's peak obtained in case (a) is of advantage.

factor has unit or higher value. The densifier indeed makes the difference between Fizeau and hypertelescope images, the former being a special case of the latter where the pupil densification factor is unit (Michelson's 20 feet interferometer had an embryonic form of pupil densification which reduced the number of fringes within the diffractive envelope, while intensifying them). An aperture synthesis observation is achieved (Fig. 2) by unmasking pairs of apertures, and adding in the computer the corresponding exposures thus made in succession with all possible pairs.

For a fair comparison of the signal/noise ratio obtained with both methods, we must also have equal collecting areas, providing the same total number of photons during observing sessions having the same duration. This would be achievable with larger pair-wise sub-apertures, and the cost of the mirrors would be comparable. However, for convenience in comparing the direct images obtained with the multiple and the masked pair-wise apertures, we prefer to keep the same size for the sub-apertures in each case, and compensate by attenuating, as the area ratio $N/2$, the hypertelescope image with a neutral density filter. Equal observing times are then needed to obtain direct or aperture-synthesis images containing the same photon count. In real future instruments, no neutral density will be used, and a pair of apertures should obviously be larger than many ones for equal photon count per hour.

As discussed elsewhere (Lardière et al. [4]), the hypertelescope exposure gives a direct image of any object, smaller than the 'Direct Imaging Field', through a pseudo-convolution of its intensity pattern with the interference function (Fig. 2).

For aperture synthesis, the pair-wise exposures obtained by masking $(N-2)$ apertures contain, across the same envelope, a fringe pattern with period and orientation depending on the pair used (Fig. 2). Exposures made in succession with all possible pairs of apertures are added in the computer, according to the principle of aperture synthesis. The added fringe patterns also generate a speckled halo. However, unlike the highly-contrasted speckled halo observed in the all-in-one exposure, the aperture-synthesis halo has faintly contrasted speckles since the fringe patterns are added incoherently as detected intensities, rather than coherently as complex amplitudes (Fig. 2). It also contains a peak, located at the same position as in the hypertelescope exposure since all fringe components have a maximum at this position. But its intensity is only twice the average speckle level since the maximal level in the elementary fringes is twice their average level. There is no 'dark zone' in the accumulated pair-wise or triplet-wise exposures since no destructive interference can occur when adding the detected exposures.

Similarly to the hypertelescope exposure, the peak is convolved if the source is resolved, and this is a way of describing how aperture-synthesis reconstructs an image, without invoking the Fourier space nor Zernike's theorem.

The scheme is nicely illustrated by the classroom demonstration of aperture synthesis by D. Wilson and J. Baldwin, mentioned in Labeyrie, Lipson and Nisenson [11], where retinal persistence is used to integrate such pair-wise images while the aperture plate is made to rotate quickly.

Two typical observing situations where it is of interest to compare the sensitivity of both approaches are: (i) the detection of a faint stellar companion located within lambda/s from a point star, possibly with a coronagraphic attachment; and (ii) the detection of a faint star amidst a uniform sky background. In both situations, photon noise is the real limitation as we assume perfect phasing and a photon-limited camera. Other forms of noise, such as the noise-like speckle pattern in the hypertelescope halo, can be removed in part by deconvolution with the calculated or calibrated spread function, although not if there is a coronagraphic attachment destroying the convolution relation. Here we will consider only the first situation.

4.1. Companion detection

In both cases, all-in-one and pairwise combination, the signal/noise ratio defining the detectability of a faint companion's peak amidst the speckled halo of the star is

$$\mathrm{SNR} = P_{\mathrm{peak}}/\sqrt{(P_h)}$$

where P_{peak} and $P_h = P_t/R$ are the total photon counts per resel or speckle in the peak and in the average halo. P_t is the total number of photons detected during the observation, and R is the number of speckles or resels, amounting to $R = (d/D)^2$ for Fizeau combination, to N for fully-densified periodic arrays, and to $(d/(D\gamma d))^2$ for non-redundant densified arrays.

In both cases, image deconvolution can improve somewhat the image quality, if not the detection sensitivity, especially in the absence of substantial pupil densification. With the CLEAN algorithm for example, the known spread function is subtracted from the image, and again subtracted from the residue, with appropriate translation. But, as remarked by Nakajima [8], this is a non-linear process where noise is difficult to calculate. We therefore only discuss the direct detection of companion peaks in both cases.

4.1.1. Signal and photon noise for all-in-one combination

For an all-in-one combination, the star peak's level is $N P_h$ and its average halo level in the dark zone is $k_d P_h$, where k_d is the darkening factor, describing the attenuation in the part of the dark zone considered. Its value is one in the pairwise case, and becomes much smaller in the hypertelescope case if there are many sub-apertures. According to Lardière et al. [4],

$$k_d = (s/D)^3 = 0.6N^{-3/2}$$

With many apertures, however, the low k_d value given by this expression is easily degraded by small piston errors. In the absence of such errors, however, k_d can be further attenuated in principle with many apertures suitably arrayed for apodizing the global aperture or with coronagraphy.

The corresponding signal/noise ratio is thus:

$$\begin{aligned}\mathrm{SNR}_h &= P_{\mathrm{peak}}/\sqrt{(k_d P_h)} = N P_h/\sqrt{(k_d P_h)} = N\sqrt{(P_h/k_d)} \\ &= N\sqrt{\big(P_t/(k_d R)\big)} = N P_t^{1/2} k d^{-1/2} R^{-1/2} = 1.4 N^{7/4} P_t^{1/2} R^{-1/2}\end{aligned}$$

For a periodic fully densified pupil, $R = N$ and therefore

$$\mathrm{SNR}_h = \sqrt{(N P_t/k_d)} = 1.29 N^{5/4} P_t^{1/2}$$

The inverse of this ratio is also the limiting relative luminosity of a faint stellar companion when its peak is just detected amidst the noisy halo.

We have considered the photon noise associated with the average halo level in the zone where the companion's peak is located. However, this peak is much better detected if coinciding with a dark speckle of the star, and, conversely, less favorably detected if the speckle is bright. This sensitivity fluctuation becomes uniformized if the speckle pattern is varied during the exposure, for example by letting the Earth's rotation vary the pupil, or by deliberately moving the apertures. This smooths the integrated speckle pattern.

4.1.2. Signal and photon noise for aperture synthesis

In the aperture-synthesis case, the summed exposure pattern obtained on a point star is also a spread function, or a pseudo spread function if the pupil is densified, which can be calibrated or calculated. A faint companion's peak is similarly detectable in the star's speckled halo, having the same average level P_h, if its intensity exceeds the photon noise.

Since the peak level is $2P_h$ in this case, the pairwise signal/noise ratio is:

$$\mathrm{SNR}_p = 2P_h/\sqrt{}(P_h) = 2\sqrt{}(P_h) = 2\sqrt{}(P_t/N)$$

if the pupil is densified like that considered in the all-on-one case.

We conjecture that equivalent results are provided by different aperture synthesis methods, using other fringe detection schemes or data reduction algorithms with pairwise incoherent exposures. It would be of interest to assess the conjecture with simulations. It should be remarked that the data reduction at radio interferometers having many antennas with heterodyne receivers, like the Very Large Array and the future Atacama Large Millimeter Array is coherent, and thus analogous to the hypertelescope case, not to the pairwise aperture synthesis achievable at visible wavelengths, where the pairwise exposures are incoherent in the absence of heterodyne detection.

4.1.3. Sensitivity gain of the hypertelescope with respect to aperture synthesis

Thus, assuming the validity of the conjecture made, the gain in dynamic range for companion detection, when doing all-in-one beam combination, is:

$$g_h = \mathrm{SNR}_h/\mathrm{SNR}_p = \sqrt{}(N P_t/k_d)/2\sqrt{}(P_t/N) = N/\big(2\sqrt{}(k_d)\big) = 0.64N^{7/4}$$

More apertures of smaller size thus greatly improve the detection sensitivity for faint companions. With $N = 1000$ sub-apertures for example, attenuating the dark zone as $k_d = 1.9 \times 10^{-5}$, companions 115 000 times, or 12.5 magnitudes, fainter can be detected with the hypertelescope. With aperture synthesis, a pair of apertures meeting the 'fair comparison' condition of equal collecting area has diameters 23 times larger than the 1000 apertures of the hypertelescope. 1000 mirrors of 1 m, arranged as a hypertelescope, thus improve the dynamic range 115 000 times with respect to a pair of 23 m ELTs using aperture synthesis. In practice, one of the ELTs should be mobile, while the 1000 apertures can be fixed. The science production when observing faint and complex objects should approximately vary as the maximal number N^2 of active resels (for example stars in a cluster) which can be imaged simultaneously, and as the signal/photon noise ratio calculated in Section 4.1.1, proportional to $N^{(5/4)}\,P_t^{(1/2)}$. P_t, the total number of photons detected during the observation, varies as the collecting area $A = Nd^2$. The signal/photon noise ratio therefore varies as $N^{(7/4)}d$, and the product describing science as $S = N^{(15/4)}d$. The cost of the primary array can be coarsely evaluated to vary as $C_{pa} = Nd^{2.5} = Ad^{0.5}$. By eliminating N between both expressions, the amount of science is thus found to vary as: $S = C_{pa}^{3.75}d^{-8.4} = A^{3.75}d^{-6.52}$. It is highly sensitive to the size of the primary sub-apertures, thus favoring a large number of small mirrors.

5. Coronagraphy with pairs versus hypertelescope

For the infra-red coronagraphic detection of exoplanets, the comparison of hypertelescopes with Bracewell nulling interferometry has been discussed by Boccaletti et al. [23]. Here, the optical scheme used for our comparison can be expanded by inserting a Lyot coronagraph between the Fizeau or hypertelescope focus and the camera. As apertures are masked for aperture-synthesis, leaving only two of them, the arrangement becomes equivalent to a Bracewell nuller, using a beam-splitter, as considered for DARWIN and TPF-I. Indeed, the focal occultor mask may then be made in the form of a phase grating having twice the period of the Fizeau fringes, and a size matching the envelope. With a grating having a square phase profile, with π amplitude, centered on the dark fringes, both transmitted beams are nulled, their energy being diffracted into higher orders which can be masked by the Lyot stop if its size is adjusted to match the baseline used (Fig. 3).

The planet's fringe pattern is offset on the grating mask, and therefore generally escapes full nulling as it is reimaged on the camera. For a synthetic-aperture reconstruction of the star's environment, the same pair-wise masking sequence is used, with matched grating and Lyot stop in each case. High-resolution peaks of several planets may thus appear directly in the long exposure achieved during the process. The associated speckled background of planet light can be partially removed with CLEAN or other deconvolution algorithms, unlike the star's residual speckles, for

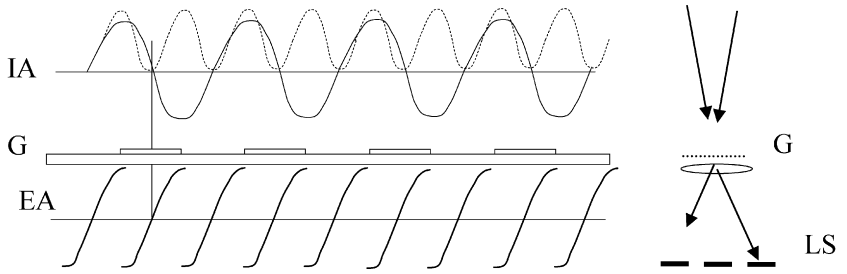

Fig. 3. Pair-wise coronagraphy with phase grating serving as occultor of two-aperture fringes in a Fizeau focal plane. The incoming complex amplitude distribution IA across the fringes (full line) has twice the period of the intensity distribution (dotted line). A transmissive phase grating G with the same double period, producing π phase shifts and positioned as indicated, reshapes the complex amplitude profile (EA). In the far-field, light is deflected in higher grating orders (right), where it can be masked by a two-aperture Lyot stop LS matching the relayed pupil pair. Off-set fringes from a planetary companion only suffer a partial attenuation. This is equivalent to the beam-splitter arrangement of Bracewell nulling, and allows building a synthetic-aperture image of the circumstellar features by switching baselines and adding exposures, using a matched grating and Lyot stop in each case.

which the coherent or incoherent cleaning methods of extreme coronagraphy are applicable (Labeyrie, Lipson and Nisenson [11]). Similar aperture synthesis is, in principle, also achievable with a Bracewell nuller if the visibility and phase of planet fringes are measured, preferably using both beams emerging from the beam-splitter.

For the hypertelescope exposure an ordinary focal occultor and Lyot mask are used if the pupil is periodic and fully densified, thus resembling that of an ELT. If not, a matching occultor and Lyot stop are needed. In terms of signal/noise ratio, the hypertelescope gain calculated in Section 4 also applies to the coronagraphic images obtained directly. Here the halo is, however, also contaminated by residual starlight, which may have the same level in both cases if resulting from weak phase disturbances, in the form of mirror bumpiness, tip-tilt and piston errors. In both cases these star residues can be attenuated with the adaptive methods of extreme coronagraphy (Trauger and Traub [13], Codona and Angel [14], Labeyrie [15]), but the more intense peak of a planet, in the hypertelescope case, makes it more easily detected.

6. Limiting magnitude of ELTs and hypertelescopes compared

6.1. With adaptive optics

We have seen in Section 3.2 that there is an advantage, regarding image crowding, in having more apertures of smaller size, at given collecting area. When imaging, with perfect phasing, a faint star against a uniform sky background, similar reasoning shows that it's limiting magnitude is invariant with respect to sub-aperture motion. Indeed, it may be assumed that an ELT pupil is 'exploded'. While its mirrors separate and keep moving outward, the Fizeau image of a point source has a constant envelope surrounding its peak, but the speckles become smaller. The central peak keeps a constant intensity, but becomes more narrow and thus contains less energy. The sky contribution may be treated as an incoherent sum of contributions from each sub-aperture, in the form of envelopes containing the energy received from a sky patch of size lambda/d. Its level within the envelope is invariant, and the (star peak)/sky ratio is therefore invariant, and equals the value with the compact ELT. The star/sky ratio in the image is also invariant when varying the size of sub-apertures, at constant global area, as discussed in Boccaletti et al. [12].

Densifying the exit pupil does not affect the peak/sky ratio but intensifies both levels as the shrinking envelope concentrates its energy into fewer resels. Doing it while the entrance aperture is being 'exploded', for maintaining a compact exit pupil, thus conserves the energy content within the peak, as well as the sky energy per resel in the envelope, and its photon noise level. Indeed, assuming for example a periodic array where the exit pupil is kept fully densified, the sky energy in the image envelope is proportional to $(\lambda/d)^2$, and each of its N resels contains $(\lambda/d)^2/N = (\pi/4)\lambda^2/A$, if $A = \pi d^2 N/4$ is again the constant collecting area. The photon noise in the sky resel is therefore proportional to $\lambda A^{1/2}$ and invariant like the photon content of the star's peak, and therefore as well as their inverse ratio which is the signal/noise ratio, determining the limiting magnitude for star detection against the sky background. We thus find that full pupil densification makes the limiting magnitude independent of the sub-aperture spacing or size. It is therefore the same as for a monolithic or ELT aperture having the same collecting area. There is a slight loss for non-periodic apertures since their exit pupil cannot be completely densified.

6.2. Without adaptive optics, using speckle interferometry

In the presence of seeing and without adaptive optics, the hypertelescope image contains 'boiling' speckles which can be exploited through speckle interferometry and its imaging variants, particularly triple correlation. The limiting magnitude is the same as for speckle interferometry in monolithic telescopes if the optics is similarly coherenced, particularly if the piston errors are dominated by the atmosphere rather than by mirror positioning. Then, the spectral filtering needed can be rather broad and the photon collection rather efficient, especially if multiple spectral channels are exploited.

Achieving adequate coherencing among the mirrors, with sub-micrometer accuracy, proved possible with the Carlina-1 prototype (Le Coroller et al. [16]): the co-spherical positioning of the mirrors on their fixed rigid supports can be monitored with simple white-light fringes at the curvature center, with 0.1 micron accuracy if the fringe positions are averaged to remove the effect of turbulence. The focal optics, a two-mirror Mertz corrector, is itself figured with a similar accuracy, using diamond turning techniques. The increased amplitude of seeing phase fluctuations, with longer baselines, however, requires somewhat shorter exposures according to Von Karman's model of the atmosphere.

The signal/noise ratio of speckle interferometry has been calculated by Dainty and Greenaway [17] and Aime [18]. Their consistent results indicate that, in the faint regime where about one photon is received per short exposure matching the turbulence life time, a useful signal/noise ratio remains obtainable by exploiting the millions of exposures which can be recorded in a few hours, and in multiple spectral channels. Instead, adaptive optics needs, during the same turbulence lifetime, at least one photon per Fried's r_0 patch, i.e. about 10^5 for a 30 m ELT at visible wavelengths.

Using speckle interferometry, ELTs and hypertelescopes can therefore observe objects fainter than any usable guide star. Laser guide stars improve the situation, but before their installation on an ELT or in modified form (Labeyrie et al. [19]) on a hypertelescope, speckle interferometry can be useful.

7. Compared technical aspects of ELT and hypertelescope

Our comparisons have assumed equal observing time and collecting area, implying a pair of larger apertures for aperture synthesis than the many smaller apertures of the hypertelescope. One should preferably consider equal construction and operating costs for both instruments, but the impact on aperture sizes is not easily calculated since highly technology-dependent. Among the major components of construction costs is the total mass of low-expansion glass or SiC invested in the mirrors, proportional to its volume. If the mirror thickness is identical for the large pair of ELTs and the many small hypertelescope mirrors, then the cost should be similar, but segment asphérization and the active supports needed for ELTs, and possibly not for Carlina-type hypertelescopes, may reduce the cost of the latter. In both cases, the size of the mirror elements may be of the order of 1 m.

The absence of a pointing mount and costly delay lines, the potential use of multiple focal gondolas, independently tracking at widely spaced positions on the primary focal sphere, can also make hypertelescopes more cost-effective. However, their site development costs may be higher since the concave topography is more demanding, and may require a new access road and landscaping work. The issue of adaptive optics and laser guide stars is also critical in both cases, and practical experience with such systems will be needed to reach a correct assessment. In addition to the LIDAR scheme proposed by Townes [20] for phasing diluted arrays in the infra-red, the feasibility of the modified sodium backscatter laser scheme proposed by Labeyrie et al. [19] is a critical point which should be urgently studied.

7.1. Site prospection under way for hypertelescopes

Ideal sites for Carlina-type hypertelescopes have a crater or a narrow and deep valley oriented East–West so that the sky coverage can extend North and South of Zenith by using an elongated array, while being restricted to 3 or 4 hours in hour angle. Natural topographic features rarely match the required spherical locus within a few meters, and landscaping may be needed, unless pylons as high as 10 or 20 m can be used to carry the mirrors, but this degrades the excellent optical path stability of mirrors directly anchored to the bed-rock. Another possibility involves stretched cable structures, similar to the hamock which carries the reflective panels at the Arecibo radio-telescope. With a few vertical constraining cables, its accuracy is said to reach 4 mm. While such structures cannot be expected to ensure the positioning of each mirror with micron tolerance, as achievable with compact mirror supports anchored in bedrock,

tens of microns may prove achievable if each mirror is constrained to maintain its height above ground by a triplet of stiff cables or rods, tensioned by the elastic hamock.

The Carlina-1 prototype uses a tethered balloon to suspend the focal optics. With the three oblique cables serving to stabilize the position of its focal optics, the balloon itself can oscillate with 10 meters amplitude from its average position without inducing excessive jitter of the recorded image. The balloon can be replaced by a servo-driven kite like those currently developed for wind generators and for pulling cargo ships. The latter (www.skysails.com) are large parafoils, having a rather good glide ratio, and which consequently pull nearly vertically. Unlike balloons, the angle is little sensitive to wind fluctuations, above the minimal wind speed which is of the order of 20 km/h. Even at the best astronomical sites with little ground wind, such winds are almost always present at higher altitudes.

Certain possible sites are located at the bottom of narrow valleys which are sufficiently deep for suspending the focal package from a traversing cable. This is could be a major simplification.

7.2. Adaptive phasing and laser guide star

Hypertelescopes can be phased adaptively on bright stars. Conventional wave sensing methods can be used within each sub-aperture, with natural or laser guide stars. However, inter-aperture phasing is also needed, and achievable with piston sensing methods such as 'dispersed speckle', a multi-aperture extension of the time-honored 'dispersed fringes' sensing used since Fizeau and Michelson. This piston sensor (Borkowski et al. [21]), has spectro-imaging optics providing a spectrum of each speckle. The non-periodically channelled spectra, or 'speckled spectra' contain the piston information. Piston maps are reconstructed by Fourier analysing in three dimensions the (x, y, λ^{-1}) data cube, or with Gerchberg–Saxton iterations. With numerical simulations of the latter method applied to periodic arrays, Martinache [22] finds that at least 10 photons/exposure/aperture/spectral element are needed. A few tens of spectral elements, each about 30 nm wide, can suffice if the piston errors result predominantly from the atmosphere. If, for example, the sub-apertures are 1.5 m in size and each internally phased with a laser guide star and individual deformable mirror, the limiting magnitude for piston sensing on a star in 10 ms is expected to be $mv = 17$ if the static piston errors are small enough to use 30 nm of spectral resolution. It improves to $mv = 21$ if the sub-apertures are 8 m in size. Whether or not refined algorithms may work with fewer photons, as also mentioned in Borkowski et al. [21], remains to be investigated.

In practice, the Fizeau pupil at the densifier's entrance is a good location for actuators, triplets of which can carry tiny mirrors in each sub-pupil (Fig. 1). Their wide relative spacing facilitates the arraying of these elements, in a Fizeau pupil plane or in the relayed image of a turbulent layer, and there is no need for a continuous deformable mirror. Tip-tilt errors, sensed with conventional Shack–Hartmann optics, are corrected together with piston by the triplet actuators, but, with the discontinuous wavefront, the separate 'dispersed speckle' sensor is required for sensing piston errors.

If the size of the sub-apertures exceeds Fried's r_0 parameter, it is of interest to also correct their internal wavefront errors by making the small adaptive mirror elements themselves deformable. A laser guide star can then be used for sensing the corresponding wavefronts elements.

A critical issue, for hypertelescopes as well as for ELTs, is the loss of sky coverage resulting from the absence of a suitable reference star in some of the fields observed. This is no problem for observing planets of bright stars, but can affect the cosmology work on deep fields. In the absence of a bright guide star in the isoplanatic patch, thousands of fainter ones are usable simultaneously if available, using the multi-channel imaging scheme of Fig. 1 which exploits distinct sets of actuators in adjacent isoplanetic patches. This improves the sky coverage of adaptive optics, but it takes a laser guide star scheme capable of sensing piston errors to achieve full sky coverage in hypertelescopes. A tentative scheme is discussed in Labeyrie et al. [19].

8. Space hypertelescopes: study progress

The slow progress of NASA and ESA towards building optical arrays in space encourages ground-based astronomy institutions such as AURA, ESO, etc. to push ELT projects, in spite of the disastrous observational impact of the atmospheric inhomogeneity. Hopes for correction with adaptive optics, and laser guide stars, are becoming supported by theory and results like those obtained at Keck II. ELT proponents expect that a good correction will become achievable on the faintest deep fields, and assume that the cost of the adaptive hardware will be lower than that of space arrays.

However, space arrays should ultimately become more efficient for difficult observations such as those of exo-Earths. In addition to monolithic space telescopes equipped with extreme coronagraphs, large hypertelescopes such as the proposed Exo-Earth Imager will be needed for obtaining resolved images of these planets, of interest for searching signs of life.

The Luciola concept for a first-generation space hypertelescope is studied in our group (Labeyrie et al. [19]). Laboratory testing is under way with models of small free-flyers. These are fitted with compact solar sails and exposed to the sun, while protected from air drafts by a glass enclosure. Current efforts toward verifying the self-pointing toward the sun have been unsuccessful so far, and we consider pursuing the testing in vacuum to minimize the radiometric torques.

9. Conclusions

Among the four major paths toward larger ground-based telescopes, also usable for stellar coronagraphy, the hypertelescope has a higher resolution than a single ELT, a much better signal/noise ratio than aperture synthesis with a few ELTs, and perhaps a better cost efficiency, especially with spherical designs favoring multiple focal stations. Equipped with a multiple densifier, hypertelescopes can provide snapshot images over wide fields. The numerous small apertures, if providing the same collecting area as an ELT, greatly relax the crowding limit of interferometers having few-elements. This allows direct imaging on deep fields containing many remote galaxies, as needed for cosmology.

Full sky coverage with adaptive optics appears achievable in hypertelescopes with laser light back-scattered from the sodium layer at 90 km altitude, but this needs to be confirmed. For observing extra-solar planets, piston sensing on the parent star can enable adaptive coronagraphy, although more extreme coronagraphy is naturally expected with space versions, particularly for resolving details of exo-Earths. As large hypertelescopes require suitable concave sites, however, fewer candidate sites may be found than for ELTs and flat arrays. Further work toward a detailed comparison of the observing performance and science efficiency, among the four types of future instruments, is obviously needed before selecting a concept.

Acknowledgements

Many people have contributed to this work. I wish to thank particularly Pierre Riaud, Claude Aime, Denis Mourard, Olivier Lardière, Hervé Le Coroller, and Julien Dejonghe, and the unknown referee who identified several errors, now corrected.

References

[1] A. Labeyrie, Astron. Astrophys. Suppl. 118 (1996) 517.
[2] E. Pedretti, et al., Astron. Astrophys. Suppl. 147 (2) (2000) 285–290.
[3] S. Gillet, et al., Astron. Astrophys. 400 (1) (2003) 393–396.
[4] O. Lardière, F. Martinache, F. Patru, Monthly Not. R. Astron. Soc. 375 (2007) 977–988.
[5] F. Patru, et al., in: Advances in Stellar Interferometry, SPIE Proc. 6268 (2006), in press.
[6] H. Le Coroller, J. Dejonghe, C. Arpesella, D. Vernet, A. Labeyrie, Astron. Astrophys. (2004).
[7] A. Labeyrie, in: Second Backaskog Workshop on Extremely Large Telescopes, Proc. SPIE 5382 (2004) 205–213.
[8] T. Nakajima, Publ. Astron. Soc. Pacific 113 (2001) 1289–1299.
[9] S. Kulkarni, et al., J. Astron. Soc. Amer. A 8 (1991) 3.
[10] S.T. Ridgway, F.J. Roddier, in: Interferometry in Optical Astronomy, Proc. SPIE 4006 (2000) 940–950.
[11] A. Labeyrie, S. Lipson, P. Nisenson, An Introduction to Optical Stellar Interferometry, Cambridge Univ. Press, Cambridge, UK, 2006.
[12] A. Boccaletti, et al., Astron. Astrophys. 338 (1998) 106–110.
[13] J. Trauger, W. Traub, Amer. Astron. Soc. Meeting 209 (2007).
[14] J.L. Codona, R. Angel, Astrophys. J. 604 (2) (2004) L117–L120.
[15] A. Labeyrie, in: Astronomy with High Contrast Imaging, Nice, EAS 12 (2004).
[16] H. Le Coroller, et al., Astron. Astrophys. 426 (2) (2004) 721–728.
[17] C. Dainty, A. Greenaway, in: Proc. “High Angular Resolution Stellar Interferometry”, 1978.
[18] C. Aime, Pure Appl. Opt. 6 (1997) 1–14, Lardière, Martinache, 2007.
[19] A. Labeyrie, et al., 2007, in preparation.
[20] C.H. Townes, Astrophys. J. 565 (2002) 1376–1380.
[21] V. Borkowski, A. Labeyrie, F. Martinache, D. Peterson, Astron. Astrophys. 429 (2005) 747–753.
[22] F. Martinache, J. Opt. A 6 (2) (2004) 216–220.
[23] A. Boccaletti, P. Riaud, C. Moutou, A. Labeyrie, Icarus 145 (2000) 628–636.